Computer and Telecommunication Engineering (2023) Volume 1 Issue 1
doi: 10.54517/cte.v1i1.2319

Asia Pacific Academy of Science Pte. Ltd.

ORIGINAL RESEARCH ARTICLE

Modelling the elevation power angle spectrum of a MIMO channel

Olabode Idowu-Bismark[1,*], Oluseun Oyeleke[2], Oluwatobiloba Idowu-Bismark[3]

[1] *Department of Electrical and Information Engineering, Covenant University, Ota 112104, Nigeria*

[2] *Department of Electrical and Electronic Engineering, Nile University of Nigeria, Abuja 900001, Nigeria*

[3] *Department of Computer Science, University of Hertfordshire, AL109JD Welwyn Hatfield, United Kingdom*

*** Corresponding author:** Olabode Idowu-Bismark, idowubismarkolabode@gmail.com

ABSTRACT

Multiple-Input Multiple-Output (MIMO) channel modelling is constantly researched, and the innovation of its three-dimensional (3D) models is the introduction of the elevation domain parameters, in particular the elevation angle of arrival (EOA) and elevation angle of departure (EOD) where their power angle spectrum (PAS) and their angular spread (AS) greatly impact the 3D MIMO performance. PAS is the basic characteristic used to estimate and model angular dispersion in wireless channels. Propagating signal waves are constrained into a path having an angle within which the power is contained. One of the scenes that will have a significant effect on these parameters is the relative height between the BS and the building. They will also depend on the distance between the base station (BS) and the user equipment (UE). In this work, we investigate the effect of distance and height on the power angle spectrum of a street canyon and a high-rise scenario in the urban environment. The wireless Insite X3D ray tracing engine and a 3D digital map of the environment were used for the simulation. It is seen that the elevation power spectrum (EPS) in the elevation domain decreases with distance and height in both scenarios for the arrival and departure. The appearance of multiple peaks leads to a double-normal distribution in the arrival of the high-rise as height increases, which is a result of reflections from multiple clusters. The azimuth power spectrum (APS) in the azimuth domain also decreases with distance and height at the arrival but increases with distance and height at the departure. The result of the power angle spectrum in this work can be used for modelling angular dispersion as well as designing adaptive antennas for wireless communication.

Keywords: angular power spectrum; FD-MIMO; EPS; APS; 3D channel modelling; 5G

1. Introduction

The use of millimetre-wave massive multiple-input multiple-output (mmWave massive MIMO) antenna systems at the base station and the small cells for wireless traffic backhauling in three-dimensional (3D) formation is being made possible with the adaptive electronic beam control capability of the full-dimension MIMO (FD-MIMO)[1]. FD-MIMO provides beam control in the azimuth and elevation planes using an active antenna system (AAS), where an independent RF chain is provided for each antenna element or group of antenna elements in a 2-dimensional planar array, thereby enhancing the benefits of 3D-MIMO techniques such as three-dimension beamforming (3DBF), vertical cell sectorization, etc.[2], which are not available in the current WiMAX, HSPA+ and LTE cellular systems. 3DBF will be used for backhauling aggregate traffic from

ARTICLE INFO
Received: 27 September 2023 | Accepted: 10 November 2023 | Available online: 19 November 2023

CITATION
Idowu-Bismark O, Oyeleke O, Idowu-Bismark O. Modelling the elevation power angle spectrum of a MIMO channel. *Computer and Telecommunication Engineering* 2023; 1(1): 2319. doi: 10.54517/cte.v1i1.2319

huge users, massive machines, and millions of sensors and forwarding the same to the core network[3]. The beamforming and spatial multiplexing technologies facilitate the wireless multipoint-to-point backhaul to hook up dense small cells for data traffic evacuation. The spatiotemporal characteristics of the backhaul channels, in particular, the power angle spectrum, determine the inter-sector interference and channel capacity performance of the backhaul links, and as such, the understanding and behaviour of the APS are vital for the comparison and assessment of contestant proposals[4]. Also, as a result of research into 3D cellular propagation that shows evidence of significant signal power spray in the elevation domain at both the BS and UE[5], strong interest has evolved to extend MIMO gain into the elevation domain to harness the benefits of MIMO elevation domain mechanisms such as vertical sectorization and user-specific elevation beamforming. The unavailability of the PAS models thus creates the problem of the inability to harness the benefits of 3D-MIMO[6,7]. The result of the power angle spectrum in this work can be used for modelling angular dispersion as well as designing adaptive antennas for wireless communication.

2. Related work

Many authors[5,7,8–10] have carried out work in the PAS domain to investigate how multiple-input, multiple-output channel multipath parameters impact various wireless channel capabilities, including data rate.

Almesaeed et al.[5] highlighted the need for user-specific elevation beamforming and full-dimensional MIMO for improved network capacity. It was specified that the channel elevation parameters, such as the elevation angles, angular spread in the elevation domain, and distribution, as well as the PAS in the elevation domain, should be considered for FD-MIMO and 3D elevation beamforming performance analysis. With a ray tracing algorithm and a 3D digital map, Wang et al.[7] used a directional antenna at 2.1 GHz to investigate the PAS of the elevation angle and their distributions both at the arrival and departure of different floors in a high-rise building. The raw data are well suited for Laplace distribution. In the work of Luo et al.[8], the authors, using channel measurements, extracted the elevation angle of departure (EOD) and elevation angle of arrival (EOA) and modelled the power angle spectrum in UMa LOS and NLOS conditions. A truncated Laplacian distribution is used to fit the probability density of the raw data. Vitucci et al.[11] simulated the multiple-input, multiple-output channel model using the ray tracing technique and characterized the various channel parameters, which include the elevation angles of arrival and departure (EOA, EOD) in both line-of-sight and non-line-of-sight situations. They also obtained the deterministic estimate of the MIMO channel matrix in the frequency domain while deriving the MIMO channel capacity estimation in a variety of cases.

MIMO antenna systems performance depend on the propagation environment[12], thus Schneider et al.[13] studied the effect of two propagation environment parameters, which are the inner-cluster Angular Spread of Arrival (ASA) and the number of clusters, on the MIMO system performance, principally how they influence the changing statistics of the MIMO channel transmit and receive side correlation which affects the MIMO channel capacity. The result indicates that increment in the number of clusters and the angular spread of arrival lead to a reduction in channel mean correlation, which is expected to lead to an increase in channel capacity. Azubogu et al.[14] used the 3D Radio-wave Propagation Simulator (RPS) ray-tracing software to characterize the received signal strength and went ahead to derive the environment pathloss exponent, power delay profile, and the power angle profile at 800 MHz in Awka City, Nigeria. To the best of the authors knowledge, no research has been carried out to model the PAS for the elevation domain of the street canyon and high-rise of an urban city. In this work, we modelled the elevation power spectrum and the azimuth power spectrum of the channel for the street canyon (LOS, O2O) scenario and the high-rise (NLOS, O2I) scenario. We investigate the height and distance effects on the EPS and APS for both scenarios. The cross-correlation coefficient of the parameters was also obtained, and we show that there is a correlation between the elevation and azimuth angles,

unlike the belief that they are independent of each other.

3. Methodology

At the base station is a 4 × 4 dual-polarized MIMO uniform planar antenna array (UPA). One of the predominant frequency ranges for the 5G NR as proposed by the 3GPP TR 138 901 release 15 of 2018[15,16] is 24.25 GHz–29.5 GHz. Also, since atmospheric attenuation for the mm wave is near its lowest at 28 GHz[17], a carrier frequency of 28 GHz was used in this work. The bandwidth of 100 MHz is the minimum channel bandwidth for all carrier frequencies as specified in the 3GPP release 15 standards necessitating the choice of 100 MHz bandwidth. The transmit power of 30 dBm was selected for a microcell BS. The BS is located at a height of 10 m and beam-forms to 300 small cells located on a street canyon in the first scenario and to 30 small cells vertically located on a 30-story building in the second scenario. The small cells, which act as receivers, use a 2 × 2 MIMO antenna array operating at 28 GHz carrier frequency and 100 MHz bandwidth. At the receiver, maximal ratio combining is used to model the receiver diversity, while the channel vectors of the H-matrix are used to adjust the magnitudes and phases of the MIMO antenna elements to maximize the total received power. The data set was obtained and imported into MATLAB for modelling. **Table 1** shows the various simulation parameters and their values while **Figure 1** shows the digital 3D map of the virtual environment of data collection.

Table 1. Parameters for the simulation.

Simulation parameters	Values
Carrier frequency	28 GHz
Bandwidth	100 MHz
Transmit power of BS	30 dBm
Height of BS	10 m
Small cell height in street	2.5 m
Small cell height in high rise	Various
Antenna BS	4 × 4 UPA
Small cell antenna	2 × 2
Antenna element spacing	1 wavelength
Number of max reflections	6
Max diffraction	1
Max penetration number	1

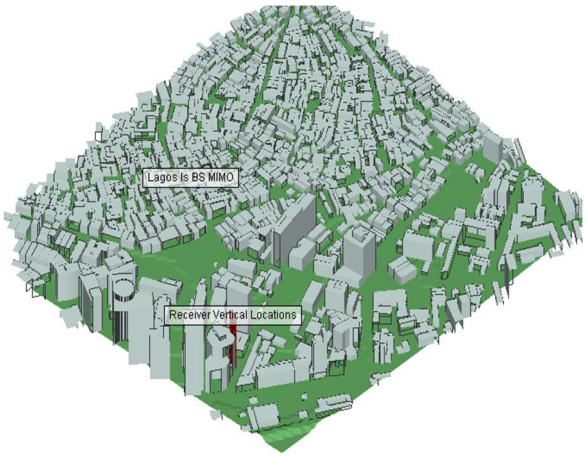

Figure 1. Digital 3D map of the virtual environment of data collection.

4. Results and discussion

The dataset of each small-scale channel parameters obtained through simulation is imported to MATLAB, 2017b to investigate the channel parameters through the characteristics of their probability distribution functions (PDFs). The author used the distribution fitter application under the statistics and machine learning toolbox to generate the appropriate best-fit PDF of the dataset. The statistics (mean and variance) of the PDF of each parameter that modelled their behaviour are then obtained. The Elevation Power Spectrum of the arrival and departure angles in the WINNER+ standardized channel model is well-fitted by the wrapped normal distribution or Laplace distribution, while the obtained results from this work are discussed below.

4.1. EPS of high-rise

The EPS of elevation angle of arrival (EOA) (at the small cells) and the EPS of elevation angle of departure (EOD) (at the BS) for the high-rise 7th floor are fitted for lognormal distribution with arriving and departing signals from a single cluster, as seen in **Figures 2** and **3**.

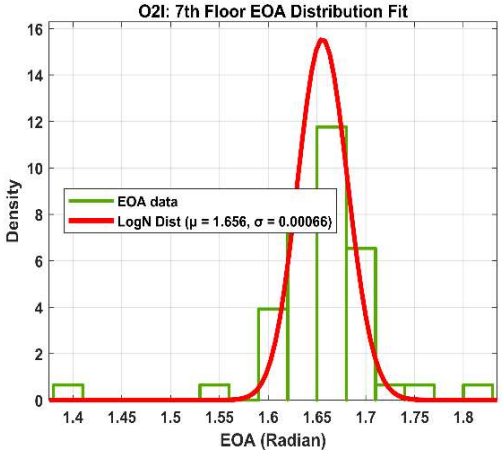

Figure 2. EPS of EOA for high-rise 7th floor.

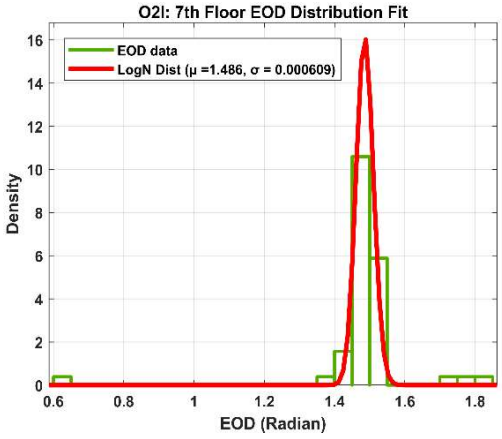

Figure 3. EPS of EOD for high-rise 7th floor.

We noticed that as the height of the building increases there appeared multiple signal clusters, as seen in **Figure 4** for the 20th floor EPS of EOA and **Figure 5** for the 26th floor EPS of EOD.

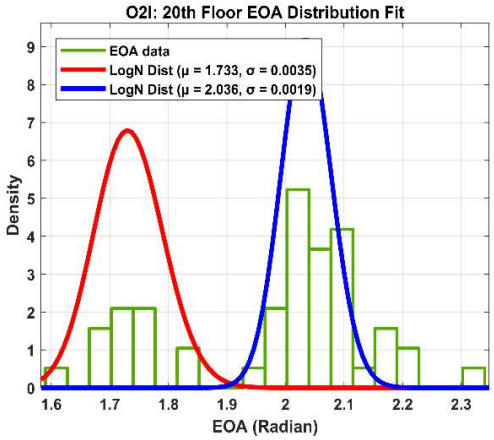

Figure 4. EPS of EOA for high-rise 20th floor.

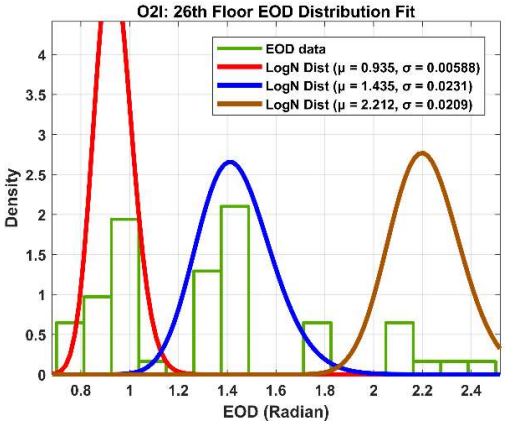

Figure 5. EPS of EOD for high-rise 26th floor.

4.2. EPS of street canyon

Observations in the street canyon scenario are different from the high-rise scenario. **Figure 6** and **Figure 7** show the EPS of EOA and EPS of EOD respectively for SC at 10 m location.

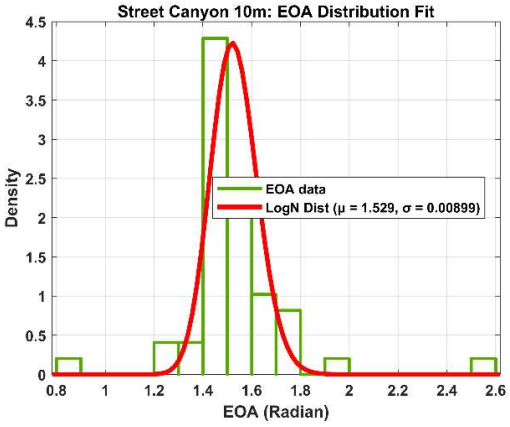

Figure 6. EPS of EOA for street canyon 10 m.

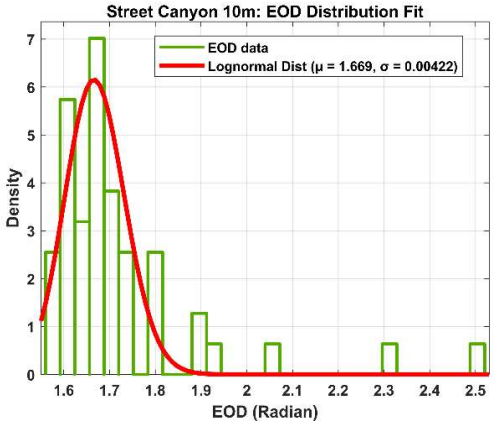

Figure 7. EPS of EOD for street canyon 10 m.

We noticed a steady decrease in the incident angles of the contained signal as the distance increases, this is seen from the EPS of EOA and EPS of EOD for SC at 170 m location as shown in **Figures 8** and **9** respectively. Our models are well-fitted with lognormal distribution.

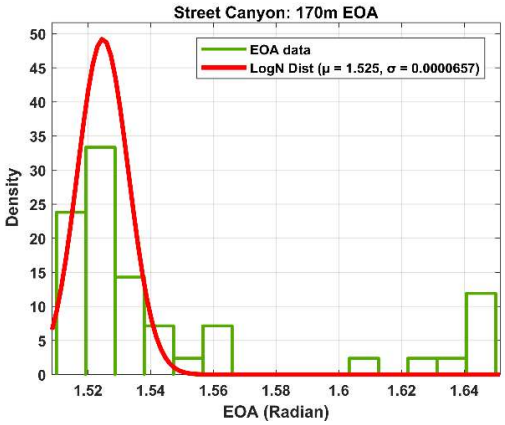

Figure 8. EPS of EOA for street canyon 170 m.

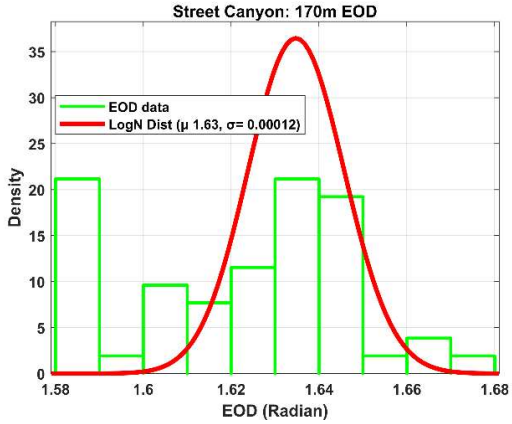

Figure 9. EPS of EOD for street canyon 170 m.

When we compare our observations at the high-rise with the observations at the street canyon, we notice the appearance of multiple peaks in the high-rise scenario as the height of the building increases while the incident angle of each peak decreases. On the other hand, an increase in distance causes a narrowing or decrease in the EPS incident angles in the street scenario. Explaining the differences in the result obtained for the EPS

of the high-rise and street canyons based on the different propagation environments, we see that Broad Street, with a width of about 14 m and buildings ranging in height from 5 stories to 20 stories lining the sides, forms a street canyon scenario, creating a waveguide for the transmitted signal. This causes a single clustered ray to reach all receivers. In the high-rise scenario, there is a disappearance of LOS rays, and the arriving rays are predominantly from multiple reflections of surrounding high-rise buildings and low-rise buildings' rooftops. Rays coming from such scatterers have entirely different propagation paths and thus arrive as independent signal clusters. This is consistent with dense high-rise environments[7,18]. The statistics of the EPS for high-rise are shown in **Table 2**, while those for the street scenario are shown in **Table 3**.

Table 2. EPS statistics for high-rise scenario.

	EPS of AOA at SC			**EPS of AOD at BS**		
Floor	μ	σ	**pdf**	μ	σ	**pdf**
7th	1.66	0.001	Lognormal	1.53	0.01	Normal
15th	1.91	0.06	Lognormal	1.27	0.11	Normal
25th	2.21 1.77	0.07 0.04	Double-lognormal	1.21 -	0.26 -	Normal
30th	1.80 2.32	0.04 0.10		2.86 2.40	0.15 0.42	
WINNER+: EPS of AOA and AOD are Laplacian or double exponential						

Table 3. EPS statistics for street scenario.

	Arrival EPS at SC			**Departure EPS at BS**		
Distance	μ	σ	**pdf**	μ	σ	**pdf**
30 m	1.49	0.08	Lognormal	1.65	0.06	Lognormal
60 m	1.49	0.004	Lognormal	1.66	0.04	Lognormal
90 m	1.53	0.084	Normal	1.65	0.07	Lognormal
330 m	1.53	0.019	Normal	1.59	0.04	Lognormal
WINNER+: EPS of AOA and AOD are Laplacian or double exponential						

When we consider the behaviour of the containing angles of the EPS for both scenarios using different floors and distance locations, as shown in **Tables 4** and **5**, we see a general decrease in the angles as height and distance increase. On the other hand, an increase in distance causes a decrease in the incident angles of the arrival and departure rays in the street scenario, which is a result of the elevation domain being bound by the ground. Also, the elevation angles in the street canyon scenario are much smaller and decrease more rapidly than the elevation angles of the high-rise. This is because the orientation of the building surfaces in the vertical domain causes them to have less effect on the reduction of the elevation angles, unlike the ground surface, which has a strong reduction effect on the elevation angles as distance increases. This is consistent with results from other authors who carried out elevation angle research[8,19,20].

Table 4. Containing angle of EOA/EOD energy for high-rise.

Floors	**Containing angle of EOA energy**	**Containing angle of EOD energy**	**pdf**
10th	17.19°	14.32°	Lognormal, Lognormal
20th	5.73°, 8.59°	17.19°, 11.46°	Lognormal, Lognormal
30th	5.73°, 11.46°	11.46°, 5.73°	Lognormal, Lognormal

Table 5. Containing angle of EOA/EOD energy for street canyon.

Distance	Containing angle of EOA energy	Containing angle of EOD energy	pdf
30 m	11.46°	11.46°	Lognormal, Lognormal
90 m	5.73°	8.59°	Lognormal, Lognormal
150 m	3.44°	1.43°	Lognormal, Lognormal

4.3. Cross-correlation

Investigating the spatial relationship between the elevation and azimuth angles and their respective power spectra. Using the 5th floor of the high-rise as a sample of 3D channel dispersion in the O2I scenario, the distribution of signal strength in the arrival (SC) and the departure (BS) are shown in **Figures 10** and **11**, respectively. We see clearly that the signal propagated in 3D space, i.e., not only in the azimuth plane but also in the elevation plane. The colour markers show the strength of the signal MPC. This same description is witnessed for the street scenario in **Figures 12** and **13** respectively using SC at a location of 30 m as a sample receiver.

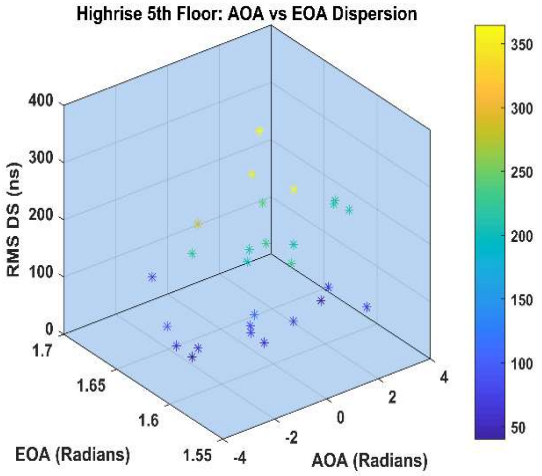

Figure 10. High-rise angular dispersion at arrival.

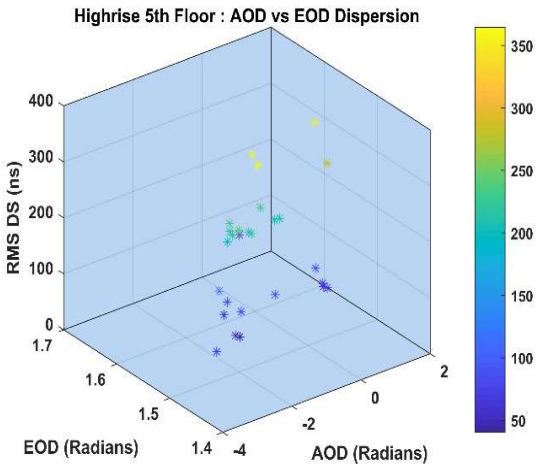

Figure 11. High-rise angular dispersion at departure.

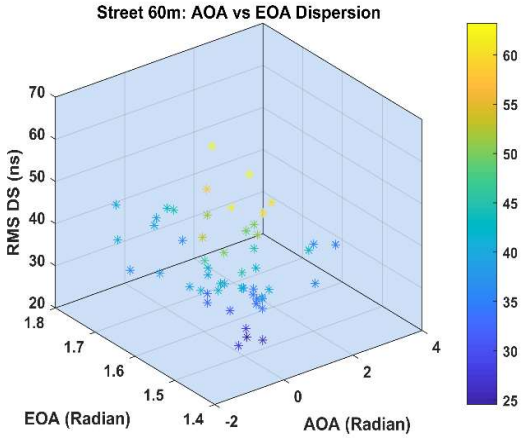

Figure 12. Street angular dispersion at arrival.

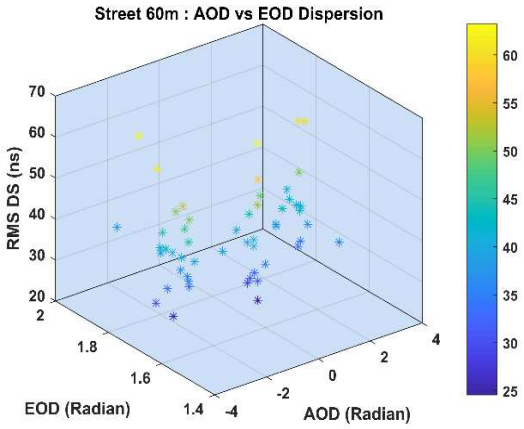

Figure 13. Street angular dispersion at departure.

5. Conclusion

In this paper, the authors modelled the power angle spectrum of the street canyon and high-rise building for the elevation domain. The PAS of the incident angle in the elevation domain decreases with distance/height in both scenarios. The simulation results show that the raw data is well fitted for a lognormal distribution in both scenarios, while the appearance of multiple peaks is observed in the high-rise scenario as height increases, which is a result of reflections from multiple clusters. The correlation diagram of the azimuth and elevation domain signals shows the existence of the elevation domain signals and their corresponding angles, which can be used in the design of directional antennas. The result of the power angle spectrum in this work can also be used for modelling angular dispersion in wireless communication.

Author contributions

Conceptualization, OIB (Olabode Idowu-Bismark); methodology, OIB (Olabode Idowu-Bismark); software, OIB (Olabode Idowu-Bismark) and OIB (Oluwatobiloba Idowu-Bismark); validation, OIB (Olabode Idowu-Bismark) and OO; formal analysis, OO; investigation, OIB (Olabode Idowu-Bismark); resources, OIB (Olabode Idowu-Bismark); data curation, OIB (Oluwatobiloba Idowu-Bismark); writing—original draft preparation, OIB (Olabode Idowu-Bismark); writing—review and editing, OIB (Olabode Idowu-Bismark); visualization, OIB (Oluwatobiloba Idowu-Bismark) supervision, OIB (Olabode Idowu-Bismark); project administration, OIB (Olabode Idowu-Bismark); funding acquisition, OIB (Olabode Idowu-Bismark). All

authors have read and agreed to the published version of the manuscript.

Acknowledgments

This work was supported by the IoT-Enabled Smart and Connected Communities (SmartCU) Research Cluster of Covenant University, the Covenant University Centre for Research, Innovation, and Discovery (CUCRID), Nigeria, and REMCOM Corporation State College, PA 16801 USA.

Conflict of interest

The authors declare that they have no conflict of interest.

References

1. Idowu-Bismark O, Kennedy O, Husbands R, Adedokun M. 5G wireless communication network architecture and its key enabling technologies. *International Review of Aerospace Engineering* 2019; 12(2): 70–82. doi: 10.15866/irease.v12i2.15461
2. Kammoun A, Alouini MS. Elevation beamforming with full dimension MIMO architectures in 5G systems: A tutorial. *IEEE Communications Surveys & Tutorials* 2019; 21(4): 3238–3273. doi: 10.1109/COMST.2019.2930621
3. Idowu-Bismark O, Oyeleke O, Atayero AA, Idachaba F. 5G small cell backhaul: A solution based on GSM-aided hybrid beamforming. *International Journal of Computer Network and Information Security* 2019; 11(8): 24–31. doi: 10.5815/ijcnis.2019.08.03
4. Zhang R, Jiang X, Taleb T, et al. Connecting a city by wireless backhaul: 3D spatial channel characterization and modeling perspectives. *IEEE Communications Magazine* 2017; 55(5): 62–69. doi: 10.1109/MCOM.2017.1600234
5. Almesaeed RN, Ameen AS, Mellios E, et al. 3D channel models: Principles, characteristics, and system implications. *IEEE Communications Magazine* 2017; 55(4): 152–159. doi: 10.1109/MCOM.2017.1500505
6. Almesaeed R, Ameen AS, Doufexi A, et al. A comparison study of 2D and 3D ITU channel model. In: Proceedings of the 2013 IFIP Wireless Days (WD); 13–15 November 2013; Valencia, Spain. pp. 1–7. doi: 10.1109/WD.2013.6686494
7. Wang XY, Li B, Yuan X, et al. Elevation angle research in three-dimension channel model using ray-tracing. In: Proceedings of the 2014 XXXIth URSI General Assembly and Scientific Symposium (URSI GASS); 16–23 August 2014; Beijing, China. pp. 1–4. doi: 10.1109/URSIGASS.2014.6929281
8. Luo Q, Pei F, Zhang J, Zhang M. 3D MIMO channel model based on field measurement campaign for UMa Scenario. In: Proceedings of the 2014 IEEE Wireless Communications and Networking Conference (WCNC); 6–9 April 2014; Istanbul, Turkey. pp. 171–176. doi: 10.1109/WCNC.2014.6951942
9. Gao Z, Dai L, Mi D, et al. MmWave massive-MIMO-based wireless backhaul for the 5G ultra-dense network. *IEEE Wireless Communications* 2015; 22(5): 13–21. doi: 10.1109/MWC.2015.7306533
10. Feng W, Li Y, Jin D, et al. Millimetre-wave backhaul for 5G networks: Challenges and solutions. *Sensors* 2016; 16(6): 892. doi: 10.3390/s16060892
11. Vitucci E, Degli-Esposti V, Fuschini F. MIMO channel characterization through ray tracing simulation. In: Proceedings of the 2006 First European Conference on Antennas and Propagation; 6–10 November 2006; Nice, France. pp. 1–6. doi: 10.1109/EUCAP.2006.4584732
12. Zhang P, Chen J, Yang X, et al. Recent research on massive MIMO propagation channels: A survey. *IEEE Communications Magazine* 2018; 56(12): 22–29. doi: 10.1109/MCOM.2018.1800196
13. Schneider C, Iqbal N, Thomä RS. Impact of angular spread and number of multipath clusters on MIMO channels. In: Proceedings of the 2015 IEEE 26th Annual International Symposium on Personal, Indoor, and Mobile Radio Communications (PIMRC); 30 August–2 September 2015; Hong Kong, China. pp. 512–516. doi: 10.1109/PIMRC.2015.7343353
14. Azubogu AC, Ohaneme CO, Ufoaroh SU, Nnebe SU. Ray tracing characterization of wideband propagation channel for simulation of mobile radio communications. *African Journal of Computing & ICT* 2012; 5(6): 17–23.
15. Lopez AV, Chervyakov A, Chance G, et al. Opportunities and challenges of mmWave NR. *IEEE Wireless Communications* 2019; 26(2): 4–6. doi: 10.1109/MWC.2019.8700132
16. 3rd Generation Partnership Project. *5G; Study on Channel Model for Frequencies from 0.5 to 100 GHz (3GPP TR 38.901 Version 15.0.0 Release 15)*. European Telecommunications Standards Institute; 2018.
17. Kumari MS, Kumar N. Channel model for simultaneous backhaul and access for mmWave 5G outdoor street canyon channel. *Wireless Networks* 2020; 26(8): 5997–6013. doi: 10.1007/s11276-020-02421-0
18. Idowu-Bismark O, Idachaba F, Atayero AA. Effect of UE height on 3D angular spread of correlated MIMO channel. In: Proceedings of the 2021 IEEE International Conference on Computational Intelligence and Virtual

Environments for Measurement Systems and Applications (CIVEMSA); 18–20 June 2021; Hong Kong, China. pp. 1–6. doi: 10.1109/CIVEMSA52099.2021.9493585

19. Zhang J, Pan C, Pei F, et al. Three-dimensional fading channel models: A survey of elevation angle research. *IEEE Communications Magazine* 2014; 52(6): 218–226. doi: 10.1109/MCOM.2014.6829967
20. Idowu-Bismark O, Idachaba F, Atayero AA. Fifth-generation small cell backhaul capacity enhancement and large-scale parameter effect. *International Journal of Electrical & Computer Engineering* 2023; 13(5): 5198–5208. doi: 10.11591/ijece.v13i5.pp5198-5208